Talanta 81 (2010) 1076–1080

Contents lists available at ScienceDirect

Talanta

journal homepage: www.elsevier.com/locate/talanta

The effect of the surface coverage of the phosphonic acid terminated self-assembled monolayers on the electrochemical behavior of dopamine

Min Zheng, Yu Chen*, Yiming Zhou*, Yawen Tang, Tianhong Lu

College of Chemistry and Environmental Science, Nanjing Normal University, Nanjing 210097, PR China

ARTICLE INFO

Article history:
Received 31 October 2009
Received in revised form 24 January 2010
Accepted 29 January 2010
Available online 4 February 2010

Keywords:
Surface coverage
Dopamine
Antifouling capability
Electron transfer
Kinetics

ABSTRACT

The surface coverage of 3-mercaptopropylphosphonic acid ($HS–CH_2CH_2CH_2–PO_3H_2$, MPPA) self-assembled monolayers (SAMs) on gold surface can be controlled by the dissociation degree of phosphonic acid groups ($–PO_3H_2$) in the bulk solution and adsorption time of MPPA molecules under the basic condition. Electrochemical measurements show that the low-density MPPA-SAMs modified gold electrode enhances significantly the kinetics of electron transfer of dopamine (DA), and improves the antifouling capability of modified electrode towards DA oxidation. The present results offer crucial information for design and optimization of the electrochemical sensors for DA determination.

1. Introduction

The electrochemical determination of the concentration of DA is an important issue for investigating its physiological functions and diagnosing nervous diseases due to the crucial role of DA in neurochemistry [1–12]. In order to eliminate the interference of other electro-active compounds (such as ascorbic acid and uric acid) and prevent the poison of the bare electrode by the oxidation products of DA, various modified electrodes have been constructed to investigate and detect DA, such as electrodes modified with polymers [1], self-assembled monolayers (SAMs) of thiolates [2], metal complex [3], carbon nanoparticles material [4], and so on. Among them, the electrochemical determination of DA at the SAMs modified electrodes (mainly, gold and carbon substrate electrodes) has attracted extensive attentions of several groups over the past 20 years due to the well-defined structures of SAMs and the ease of fabrication [5–12]. These investigations facilitate a fundamental understanding of the SAMs–DA interaction occurring in the electrode–solution interface (i.e. double layer region) at the molecular level due to the simplicity of the SAMs–DA system.

It is well known that the electrochemical behavior of DA on the SAMs modified electrode is strongly dependent on the thickness of the monolayer [11], the type of terminal functional group [6–9,12] and the morphology of substrate [5]. Very recently, we have reported the high-density MPPA-SAMs modified gold electrode for sensitive determination of DA in the presence of ascorbic acid, however, the modified electrode suffers from a fouling effect due to the accumulation of oxidized products [2]. Although some researchers think that the well-organized and compacted SAMs modified electrode can offer advantages such as selectivity, sensitivity and small over-potential for the determination of DA [6,7], to the best of our knowledge, the effect of the surface coverage of the SAMs on the electrochemical behavior of DA has not been reported systemically.

The aim of this work is to use cyclic voltammetry to investigate the effect of the surface coverage of the SAMs on the electrochemical behavior of DA rather than the electrochemical determination of the concentration of DA. In this report, we for the first time observed that the electrochemical behavior of DA was strongly dependent on the fractional surface coverage of the phosphonic acid terminated SAMs. The gold electrode modified with low-density MPPA-SAMs significantly enhanced the kinetics of electron transfer of DA, and improved the antifouling capability of modified electrode towards the oxidation of DA. The work provides a fundamental in understanding the SAMs–DA interaction and offers crucial information for design and optimization of the electrochemical sensors about DA determination.

2. Experimental

2.1. Materials

Dopamine (DA) was received from Sigma–Aldrich (St. Louis, USA) and used without further purification. 3-Mercaptopropyl-

* Corresponding authors. Tel.: +86 25 85891651; fax: +86 25 83243286.
E-mail addresses: ndchenyu@yahoo.cn (Y. Chen), zhouyiming@njnu.edu.cn (Y. Zhou).

0039-9140/$ – see front matter © 2010 Elsevier B.V. All rights reserved.
doi:10.1016/j.talanta.2010.01.063

phosphonic acid (HS–$CH_2CH_2CH_2$–PO_3H_2, MPPA) was synthesized according to literature [2]. The other chemicals were of analytical grade (AR). All the aqueous solutions were prepared with Millipore water having a resistivity of 18.2 MΩ (Purelab Classic Corp., USA). 0.1 M phosphate buffer solution (PBS, pH 7.4) was prepared by using Na_2HPO_4 and NaH_2PO_4. Freshly prepared DA solution was used in all experiments.

2.2. Apparatus

Voltammetric experiments were performed by using a CHI 660 B electrochemical analyzer (CH Instruments, Shanghai Chenhua Co.). All voltammograms were recorded with a three-electrode system consisting of a saturated calomel reference electrode (SCE), a Pt plate as the counter electrode, and the bare gold or modified gold electrodes as the working electrode. The electrolyte was purged with high-purity nitrogen for at least 10 min prior to measurements to remove dissolved oxygen. Then the electrochemical cell was kept under nitrogen atmosphere throughout the experiments. All the electrochemical experiments were carried out at room temperature (20 ± 2 °C). In all cyclic voltammetry and linear sweep voltammetry measurements, the scan rate is fixed at 100 mV s^{-1} and the supporting electrolyte is 0.1 M PBS (pH 7.4) unless otherwise stated. The formal potentials of SAMs desorption in 0.5 M KOH solution were presented by using 10 measurements for 1 sample.

The high-resolution X-ray photoelectron spectroscopy (XPS) measurements were carried out on a Thermo VG Scientific ESCALAB 250 spectrometer with a monochromatic Al Kα X-ray source (1486.6 eV photons), and the vacuum in the analysis chamber was maintained at about 10^{-9} mbar or lower. Power of the X-ray source was kept constant at 150 W. The binding energy was calibrated by means of the Au $4f_{7/2}$ peak energy of 84.0 eV. The curves were fitted by using the XPSPEAK41 software.

2.3. Preparation of MPPA-SAMs modified electrodes

Before deposition of MPPA-SAMs, a gold electrode (CHI, 2 mm in diameter) was pretreated by the oxidation/reduction cycling in a 0.5 M H_2SO_4 solution [13]. Then, the pretreated electrode was immersed in a solution of 4 mM MPPA + 0.1 M $HClO_4$ for 24 h, or a solution of 4 mM MPPA + 0.1 M KOH for 24 h, or a solution of 4 mM MPPA + 0.1 M KOH for 15 min at room temperature. After the electrode was rinsed with the same base–acid rinse protocol [14] (i.e. the electrode was rinsed consecutively with Millipore water, 0.1 M KOH, 0.1 M $HClO_4$, and Millipore water, respectively), the resulting electrode was denoted as the MPPA-H/Au, MPPA-M/Au and MPPA-L/Au electrode, respectively.

3. Results and discussion

3.1. Preparation of MPPA-SAMs

In our previous work [14], the base–acid rinse protocol has been presented to prepare the MPPA monolayers free of unbound MPPA thiols. As revealed by the XPS measurements (Fig. 1A), only doublet peaks of bound MPPA thiolates ($S_{2p3/2}$: 162.0 eV and $S_{2p1/2}$: 163.2 eV) are observed in each S_{2p} spectrum, and no trace of the peaks associated with K^+ ions ($K_{2p3/2}$: 292.9 eV and $K_{2p1/2}$: 297.0 eV) are observed in the K_{2p} region (290–300 eV), indicating that all three electrodes contain completely protonated monolayers of MPPA [14]. The difference in surface coverage of MPPA-SAMs at the three electrodes is confirmed by XPS and electrochemical desorption measurements. XPS scans of the S_{2p} region show that the peak intensity of S_{2p} at the MPPA-H/Au electrode is 1.3 and 2 times larger than that at the MPPA-M/Au and MPPA-L/Au electrode, respectively (Fig. 1A), which demonstrates that the order of

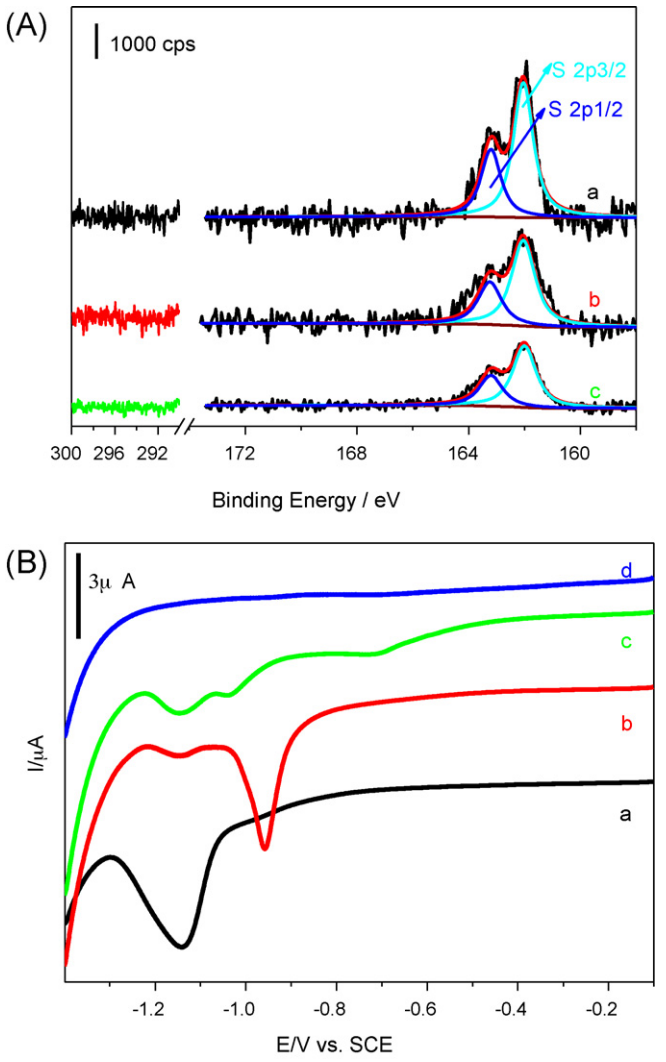

Fig. 1. (A) XPS spectra of (a) the MPPA-H/Au, (b) the MPPA-M/Au and (c) the MPPA-L/Au electrodes in the K_{2p} region and S_{2p} region. (B) Linear sweep voltammograms of (a) the MPPA-H/Au, (b) the MPPA-M/Au, (c) the MPPA-L/Au and (d) the bare gold electrodes in 0.5 M KOH at scan rate of 100 mV s^{-1}.

the surface coverage of the MPPA-SAMs at the different electrodes is MPPA-H/Au > MPPA-M/Au and MPPA-L/Au electrode.

The difference in surface coverage of MPPA-SAMs at these three electrodes is confirmed by the electrochemical desorption measurements of the SAMs in 0.5 M KOH solution. As shown in Fig. 1B, the MPPA-H/Au electrode show one clear desorption peak located around −1.13 ± 0.02 V and a very small peak located at −0.95 ± 0.03 V. The appearance of small peak can be explained by the presence of a disordered phase of MPPA-SAMs at the step and domain boundaries [15–18]. For comparison, the MPPA-M/Au shows two clear desorption peaks (about −1.13 ± 0.02 and −0.95 ± 0.03 V), and the MPPA-L/Au electrode shows three clear desorption peaks (about −1.15 ± 0.02, −0.99 ± 0.04 and −0.7 ± 0.03 V). The observations demonstrate massive disordered phase of MPPA-SAMs exists in the surface of MPPA-M/Au and MPPA-L/Au electrodes. It is clear that desorption peak potential of thiolates-SAMs is also related to the compactness of the SAMs [19–22]. Compacted thiolates-SAMs always result in desorption peak potential at more negative values because densely packed SAMs are likely to be less permeable to ions than loosely packed SAMs. Thus, the distinguished difference in desorption peak potentials of MPPA-SAMs implies the order of the

compactness of the MPPA-SAMs at the different electrodes is MPPA-H/Au > MPPA-M/Au and MPPA-L/Au electrode. The reductive desorption of thiolates-SAMs on the Au surface is a one electron reaction process, and thus the surface concentration of the thiolates-SAMs can be roughly determined from the charge consumed during the reductive desorption [14]. By integrating the current under the desorption peak (Fig. 1B), the surface coverage of the MPPA-SAMs at MPPA-H/Au, MPPA-M/Au, and MPPA-L/Au electrodes are estimated to be $5.5 \pm 0.4 \times 10^{-10}$, $4.4 \pm 0.4 \times 10^{-10}$, and $2.9 \pm 0.3 \times 10^{-10}$ mol cm^{-2}, respectively. Thus, the electrochemical characterizations further indicate that the MPPA-H/Au and MPPA-L/Au electrode has highest and lowest fractional surface coverage of the MPPA-SAMs among the three electrodes, respectively.

Thus, the surface coverage of MPPA-SAMs on gold electrode can be controlled by the dissociation degree of $-PO_3H_2$ in the bulk solution. Namely, a higher dissociation degree of the phosphonic acid group results in a high charge of MPPA molecules and hence larger electrostatic repulsion between MPPA molecules on the gold surface, leading to less compacted SAMs [14]. Therefore, the MPPA-M/Au electrode prepared under the basic condition has less surface coverage of MPPA-SAMs than that of MPPA-H/Au electrode prepared under the acidic condition.

The self-assembly process of non-charged thiol molecule on gold surface was a two-step process: an initial fast step followed by a slow step [23–25]. During the first step, the non-charged thiol coverage quickly increases up to coverage of about 80–90% of the completed monolayer within 1–2 min. For example, Raj and Behera observed that the surface coverage for three different 6-mercaptonicotinic acid SAMs prepared at different soaking time did not change appreciably [26]. The surface coverage value for the 6-mercaptonicotinic acid SAMs prepared at 30 min, 2 h and 20 h soaking time was found to be 2.0×10^{-10}, 2.01×10^{-10} and 2.02×10^{-10} mol cm^{-2}, respectively. As the case of 6-mercaptonicotinic acid SAMs, the surface coverage of MPPA-SAMs on gold surface should be also hardly modulated by controlling adsorption time of MPPA molecules under the acidic conditions due to fast adsorption kinetics. After a pretreated gold electrode is immersed in a 4 mM MPPA solution containing 0.1 M $HClO_4$ for 15 min, the electrochemical desorption curve of MPPA-15 min/Au electrode obtained is similar to that of present MPPA-H/Au electrode (data not shown), indicating the formation of MPPA-SAMs on gold surface is rather fast under the acidic condition.

In the previous works, Bard and co-workers [27,28] have found that the self-assembly process of charged thiol on gold surface was also a two-step process. However, the initial step was completed within about 150 min, indicating the adsorption kinetics of charged thiol molecules on gold surface was very sluggish compared to non-charged thiol molecules. Once MPPA-SAMs were prepared under the strong basic condition, similar phenomenon was also observed in our present works. As revealed by the XPS and electrochemical desorption measurements (Fig. 1), the surface coverage of MPPA-SAMs at the MPPA-L/Au electrode is much lower than that of MPPA-M/Au electrode, indicating that adsorption kinetics of MPPA molecules is sluggish under the basic condition. The present observations indicate that solution pH affect considerably the adsorption kinetics of MPPA molecules. Under the acidic condition, the interchain hydrophobic interaction of neutral MPPA molecules is favorable for the self-assembling process. On the contrary, under the basic condition, the repulsive interaction between adsorbed negatively charged MPPA is responsible for the sluggish adsorption kinetics of MPPA molecules on gold surface [27]. As a result, the surface coverage of MPPA-SAMs on gold surface can further be modulated conveniently by controlling adsorption time of MPPA molecules under the basic condition due to its sluggish adsorption kinetics.

3.2. Electrochemistry of DA on the MPPA-SAMs

In our previous works [2], $Fe(CN)_6^{3-}$ and $Ru(NH_3)_6^{3+}$ redox probe molecules, carrying oppositely charge, have been used to investigate systematically the interface properties of the MPPA-SAMs modified electrode. It was observed that the electron transfer of $Fe(CN)_6^{3-}$ was completely blocked at the MPPA-SAMs modified electrode due to electrostatic repulsion, whereas no blocking effects occurred for $Ru(NH_3)_6^{3+}$ at the MPPA-SAMs modified electrode compared with the bare gold electrode due to electrostatic attraction. It is clear that the DA molecule is protonated and positively charged under physiological pH conditions, whereas $-PO_3H_2$ in MPPA-SAMs are negatively charged under this pH value [2,14]. Thus, as the case of $Ru(NH_3)_6^{3+}$, positively charged DA is expected to accumulate on the MPPA-SAMs modified electrode surface with negative charges through the electrostatic and/or hydrogen-bonding interactions [2,29]. Fig. 2 shows the cyclic voltammograms of DA at the bare gold and MPPA-SAMs modified gold electrodes in 0.1 M PBS (pH 7.4). It is clearly observed that peak to peak separation (ΔE_p) of DA at MPPA-H/Au, MPPA-M/Au, MPPA-L/Au and bare gold electrode is 300 ± 20, 171 ± 10, 52 ± 8 and 75 ± 12 mV, respectively. As can be seen, ΔE_p of DA at MPPA-SAMs modified gold electrodes decreases with decreasing the surface coverage of MPPA-SAMs, accompanying with the increase of oxidation peak currents ($i_{p,a}$) and the improvement of reversibility. Since smaller ΔE_p corresponds to larger electron transfer rate [30], the ΔE_p analysis indicates that both MPPA-H/Au and MPPA-M/Au electrode suppress the kinetics of electron transfer of DA whereas MPPA-L/Au electrode facilities the kinetics of electron transfer of DA compared with the bare gold electrode.

For DA oxidation at SAMs modified electrodes, Mandler [11] suggested that two factors including the charge of the SAMs and the length of the carbon chain were likely to govern the electron transfer kinetics of DA. Thus, the electrostatic interactions between DA and $-PO_3H_2$ in the MPPA-SAMs will facilitate electron transfer of DA due to the accumulation of DA at electrode surface, whereas the presence of carbon chain of MPPA-SAMs will inhibit electron transfer of DA due to the increase in the electron transfer distance between DA and electrode [11]. Compared with the high-density MPPA-SAMs (Insert A), the low-density MPPA-SAMs can decrease the electron transfer distance between DA and electrode due to the collapse of carbon chain (Insert B). Obviously, this

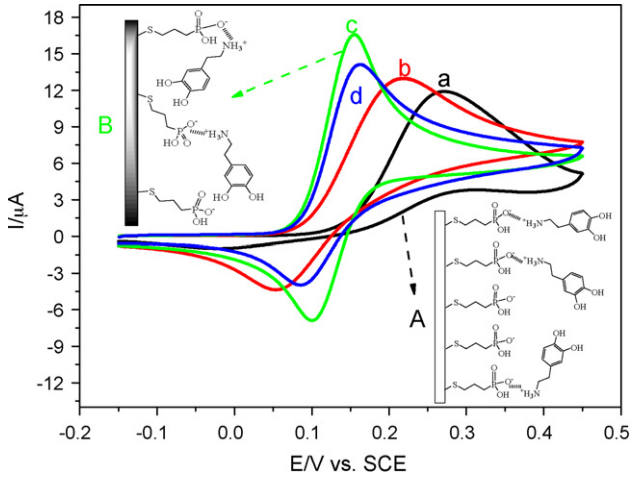

Fig. 2. Cyclic voltammograms of 1 mM DA at (a) the MPPA-H/Au, (b) the MPPA-M/Au, (c) the MPPA-L/Au and (d) the bare gold electrodes in 0.1 M PBS (pH 7.4) at scan rate of 100 mV s^{-1}. Insert: Schematic representation of the interaction between DA and MPPA-SAMs: (A) the high-density MPPA-SAMs, (B) the low-density MPPA-SAMs.

should decrease significantly the blocking effect of carbon chain length of MPPA-SAMs for DA. As a result, the positive effect of the electrostatic attraction may exceed the adverse blocking effect of MPPA-SAMs for electron transfer of DA, which results in a significant enhancement of the kinetics of electron transfer of DA at MPPA-L/Au electrode.

3.3. Antifouling capability of modified electrodes

The general mechanisms of the electrochemical behavior of DA in aqueous solution can be represented as an ECE process [31]. During the electrochemical oxidation of DA, *o*-dopaminoquinone, an oxidation product of DA, undergoes easily a ring closure reaction to form dopaminochrome. This intermediate species can polymerize to melanin-like compounds to poison electrode [7], which results in rather poor selectivity and sensitivity for determination of DA in real sample analysis. For practical electrochemical measurement of DA, the working electrode must possess a good antifouling capability. Fig. 3 shows the first and 15th voltammetric curves of DA oxidation on a bare gold and MPPA-SAMs modified gold electrodes with repeated potential scans. After 15th potential scans, $i_{p,a}$ of DA at bare Au, MPPA-H/Au, MPPA-M/Au and MPPA-L/Au electrode decrease to 65%, 85%, 96% and 96% of their initial maximum values (i.e. first scan), respectively. This result demonstrates that the fouling of the electrode surface is suppressed by the MPPA-SAMs, and the low-density MPPA-SAMs modified electrodes provide a better antifouling capability for DA oxidation.

It is clear that the surface negative charge density of MPPA-SAMs modified electrodes is higher than that of bare Au electrode, whereas the antifouling capability of MPPA-SAMs modified electrodes is much better than that of bare gold electrode. The result clearly indicates the amount of electrogenerated melanin-like compounds at the surface of MPPA-SAMs modified electrodes is lower than that of bare gold electrode after repeated potential scans. Since the formation of dopaminochrome requires the direction of the protonated side chain of *o*-dopaminoquinone towards the quinone ring [32], the electrostatic and/or hydrogen-bonding interaction between DA and $-PO_3H_2$ in the MPPA-SAMs is likely to stabilize the chain of DA, or at least to suppress its mobility, which certainly prevents the ring closure reaction of *o*-dopaminoquinone and its following reactions [32].

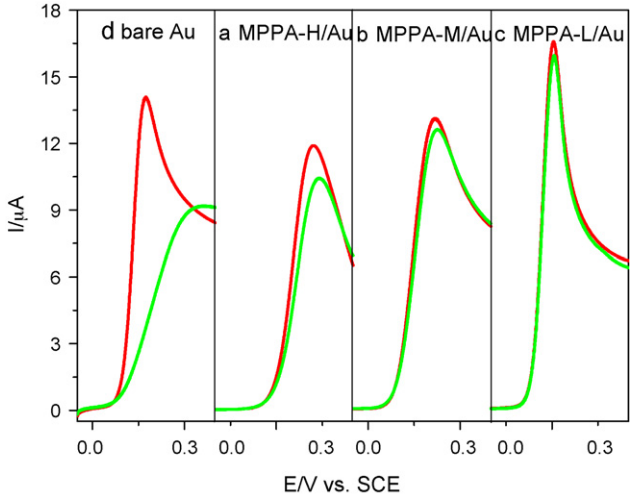

Fig. 3. Linear sweep voltammograms of 1 mM DA at (a) the MPPA-H/Au, (b) the MPPA-M/Au, (c) the MPPA-L/Au and (d) the bare gold electrodes with repeated scans in 0.1 M PBS (pH 7.4), respectively. Red line: the first scan; green line: the 15th scan. Scan rate: 100 mV s^{-1}. (For interpretation of the references to color in this figure legend, the reader is referred to the web version of the article.)

The previous reports have indicated that the measured pK_a of surface-confined acidic molecule is significantly higher than the bulk pK_a of the same molecule in solution owing to the hydrogen-bonding stabilization and the steric effect, etc. [33,34]. A recent investigation has found that the surface pK_a of mercaptopropionic acid (MPA) SAMs decreases with decrease in the surface coverage of MPA-SAMs due to a decrease of inplane interaction between –COOH groups [19]. Since both mercaptopropionic acid and MPPA are ω-substituted linear alkanethiol molecules, the pK_a of MPPA-SAMs will decrease with decreasing the surface coverage of MPPA-SAMs due to the decrease of probability of the hydrogen-bonding interaction between $-PO_3H_2$ groups, as in the case of COOH-terminated MPA-SAMs [19]. Thus, every $-PO_3H_2$ in low-density MPPA-SAMs should possess higher negatively charge unit than that in high-density MPPA-SAMs in same pH value, which in turn enhances the electrostatic and/or hydrogen-bonding interaction between DA and $-PO_3H_2$, and consequently, more effectively prevents the ring closure reaction of *o*-dopaminoquinone. Moreover, in the case of low-density MPPA-SAMs, the mobility of the protonated side chain of *o*-dopaminoquinone can been suppressed by carbon chain of MPPA thiolates due to the penetration of DA in SAMs (Insert B in Fig. 2), which facilitates also suppression of the ring closure reaction of *o*-dopaminoquinone. The above-mentioned assumptions are completely supported by cyclic voltammetry experiments (Fig. 2). Voltammetric studies involving DA oxidation usually present $i_{p,c}/i_{p,a}$ ratio smaller than 1, because DA oxidation involves an ECE mechanism and the chemical step consumes the electrooxidized DA species. However, it is interesting to find that $i_{p,c}/i_{p,a}$ ratio of DA at the MPPA-L/Au electrode is closer to 1 than that observed for bare gold electrode (Fig. 2), which strongly indicates that the chemical step is restrained at MPPA-L/Au electrode. Therefore, the MPPA-L/Au electrodes with low-density MPPA-SAMs provide a better antifouling capability for DA oxidation than that of MPPA-H/Au electrode.

4. Conclusions

For the different aims, researchers look to fabricate the SAMs with different quality. We report herein that the adsorption behavior of MPPA molecules on gold surface is actually sensitive to bulk solution pH. Consequently, the MPPA-SAMs with the different surface coverage can be prepared simply by controlling the dissociation degree of $-PO_3H_2$ in the bulk solution as well as adsorption time of MPPA molecules under the basic condition. This simple combined preparation method may afford a versatile approach to deliberately control the order of other acidic-group terminated thiolates-SAMs. Compared with its dense-density counterparts, the low-density MPPA-SAMs modified electrode enhances significantly the kinetics of electron transfer of DA oxidation, which may be attributed to the decrease of the electron transfer distance between DA and electrode due to the collapse of MPPA-SAMs. Meanwhile, low-density MPPA-SAMs modified electrodes improve also antifouling capability of modified electrode towards DA oxidation because enhanced electrostatic interaction and the penetration of DA in SAMs can more effectively prevent the ring closure reaction of *o*-dopaminoquinone by suppressing mobility of carbon chain in DA molecules. The present results provide the fundamental understanding of the SAMs–DA relationship at the molecular level and offer crucial information for design and optimization of the electrochemical sensors about DA determination.

Acknowledgment

This work is supported by the Priming Scientific Research Foundation for Advanced Talents in Nanjing Normal University.

References

[1] S.A. Kumar, C.F. Tang, S.M. Chen, Talanta 74 (2008) 860–866.
[2] Y. Chen, L.R. Guo, W. Chen, X.J. Yang, B. Jin, L.M. Zheng, X.H. Xia, Bioelectrochemistry 75 (2009) 26–31.
[3] E. Shams, A. Babaei, A.R. Taheri, M. Kooshki, Bioelectrochemistry 75 (2009) 83–88.
[4] Y. Wang, Y.M. Li, L.H. Tang, J. Lu, J.H. Li, Electrochem. Commun. 11 (2009) 889–892.
[5] J.D. Zhang, M. Oyama, Electrochem. Commun. 9 (2007) 459–464.
[6] Y. Wang, J. Luo, H.W. Chen, Q. He, N. Gan, T.H. Li, Anal. Chim. Acta 625 (2008) 180–187.
[7] L. Codognoto, E. Winter, J.A.R. Paschoal, H.B. Suffredini, M.F. Cabral, S.A.S. Machadoc, S. Rath, Talanta 72 (2007) 427–433.
[8] H. Wang, L.J. Wang, Z.F. Shi, Y. Guo, X.P. Cao, H.L. Zhang, Electrochem. Commun. 8 (2006) 1779–1783.
[9] Y.X. Sun, S.F. Wang, Microchim. Acta 154 (2006) 115–121.
[10] Y. Li, X. Huang, Y. Chen, L. Wang, X. Lin, Microchim. Acta 164 (2009) 107–112.
[11] F. Malem, D. Mandler, Anal. Chem. 65 (1993) 37–41.
[12] A. Dalmia, C.C. Liu, R.F. Savinell, J. Electroanal. Chem. 430 (1997) 205–214.
[13] Y. Chen, B. Jin, L.R. Guo, X.J. Yang, L.M. Zheng, X.H. Xia, Chem. Eur. J. 14 (2008) 10727–10734.
[14] Y. Chen, X.J. Yang, B. Jin, L.R. Guo, L.M. Zheng, X.H. Xia, J. Phys. Chem. C 113 (2009) 4515–4521.
[15] T. Kawaguchi, H. Yasuda, K. Shimazu, M.D. Porter, Langmuir 16 (2000) 9830–9840.
[16] D.F. Yang, C.P. Wilde, M. Morin, Langmuir 12 (1996) 6570–6577.
[17] I. Thom, M. Buck, Surf. Sci. 581 (2005) 33–46.
[18] J. Noh, E. Ito, K. Nakajima, J. Kim, H. Lee, M. Hara, J. Phys. Chem. B 106 (2002) 7139–7141.
[19] K. Kim, J. Kwak, J. Electroanal. Chem. 512 (2001) 83–91.
[20] D.F. Yang, C.P. Wilde, M. Morin, Langmuir 13 (1997) 243–249.
[21] J.F. Cabrita, L.M. Abrantes, A.S. Viana, Electrochim. Acta 50 (2005) 2117–2124.
[22] D. Garcıa-Raya, R. Madueno, J.M. Sevilla, M. Blazquez, T. Pineda, Electrochim. Acta 53 (2008) 8026–8033.
[23] G.E. Poirier, E.D. Pylant, Science 272 (1996) 1145–1148.
[24] G. Hahner, C. Woll, M. Buck, M. Grunze, Langmuir 9 (1993) 1955–1958.
[25] C.D. Bain, E.B. Troughton, Y.Y. Tao, J. Evall, G.M. Whitesides, R.G. Nuzzo, J. Am. Chem. Soc. 111 (1989) 321–335.
[26] C.R. Raj, S. Behera, J. Electroanal. Chem. 581 (2005) 61–69.
[27] K. Hu, A.J. Bard, Langmuir 13 (1997) 5114–5119.
[28] K. Hu, A.J. Bard, Langmuir 14 (1998) 4790–4794.
[29] C.E. Park, Y.G. Jung, J.I. Hong, Tetrahedron Lett. 39 (1998) 2353–2356.
[30] A.J. Bard, L.R. Faulkner, Electrochemical Methods: Fundamentals and Applications, Wiley, New York, 2000.
[31] N.J. Ke, S.S. Lu, S.H. Cheng, Electrochem. Commun. 8 (2006) 1514–1520.
[32] J. Weng, J. Xue, J. Wang, J. Ye, H. Cui, F. Sheu, Q. Zhang, Adv. Funct. Mater. 15 (2005) 639–647.
[33] M.L. Wallwork, D.A. Smith, J. Zhang, J. Kirkham, C. Robinson, Langmuir 17 (2001) 1126–1131.
[34] K.H. Sheikh, S.D. Evans, H.K. Christenson, Langmuir 23 (2007) 6893–6895.